M. Rossi · L. Reatto · D.E. Galli

Study of solid ^{4}He in two dimensions

The issue of zero–point defects and study of confined crystal

Abstract Defects are believed to play a fundamental role in the supersolid state of ^{4}He. We report on studies by exact Quantum Monte Carlo (QMC) simulations at zero temperature of the properties of solid ^{4}He in presence of many vacancies, up to 30 in two dimensions (2D). In all studied cases the crystalline order is stable at least as long as the concentration of vacancies is below 2.5%. In the 2D system for a small number, n_v, of vacancies such defects can be identified in the crystalline lattice and are strongly correlated with an attractive interaction. On the contrary when $n_v \gtrsim 10$ vacancies in the relaxed system disappear and in their place one finds dislocations and a revival of the Bose-Einstein condensation. Thus, *should* zero–point motion defects be present in solid ^{4}He, such defects would be dislocations and not vacancies, at least in 2D. In order to avoid using periodic boundary conditions we have studied the exact ground state of solid ^{4}He confined in a circular region by an external potential. We find that defects tend to be localized in an interfacial region of width of about 15 Å. Our computation allows to put as upper bound limit to zero–point defects the concentration 3×10^{-3} in the 2D system close to melting density.

Keywords zero–point defects · solid ^{4}He · supersolid

PACS 67.80.-s · 67.80.bd · 67.80.dj

M. Rossi
Dipartimento di Matematica, Politecnico di Milano, Piazza Leonardo da Vinci 32, 20133 Milano, Italy

L. Reatto
Dipartimento di Fisica, Università degli Studi di Milano, via Celoria 16, 20133 Milano, Italy

D.E. Galli
Dipartimento di Fisica, Università degli Studi di Milano, via Celoria 16, 20133 Milano, Italy

1 Introduction

Supersolidity is an intriguing state of matter in which spatial order, typical of the solid phase, and off-diagonal long range order [1] (ODLRO), which characterizes the Bose–Einstein condensation (BEC) phenomena, are simultaneously present, implying some form of superfluid properties even for the solid phase. This striking idea of a superfluid solid was proposed long ago [2, 3] and solid ^{4}He was early recognized as the natural candidate to display such a counterintuitive coexistence of orders. This topic attracted the attention of many physicists [4] before going out of attention in the absence of experimental evidence. As a consequence of the recent discovery of non classical rotational inertia (NCRI) [5] in solid ^{4}He, one of the expected manifestations of supersolidity [6], the possible existence of a supersolid phase has recently gained once more the attention of the scientific community, making solid ^{4}He systems the subject of many experimental and theoretical studies (See Refs. [7,8,9,10] for recent reviews).

There is strong evidence that defects play an important role in NCRI. In fact, experiments show that usually NCRI is strengthened by increasing disorder in the crystal, and microscopic simulation studies agree on the fact that an ideal perfect crystal does not show ODLRO [11,12] even at $T = 0$ K [13,9]. By *ideal perfect crystal* we mean a crystalline solid extended to all space with *one atom per lattice site*. A key question is if bulk solid ^{4}He is an ideal perfect crystal or not. For instance, if zero–point independent vacancies were present, the crystal would still be perfect because vacancies are delocalized defects, but not ideal because there would be less than one atom per lattice site (this is also called an incommensurate solid). Notice that the earlier proposal [2,3] for the supersolid state assumed the presence of zero–point defects in the ground state of solid ^{4}He in the form of ground state vacancies. Presently there is a prevalent view that supersolidity is an extrinsic property of solid ^{4}He. However not all share this view [14,9,15] and present experiments cannot rule out the presence of intrinsic defects[16,17]. Moreover, it is still not clear which kind of disorder contributes to, or is responsible for, the anomalous properties observed in solid ^{4}He. Many different defects have been considered, ranging from vacancies to grain boundaries, passing from dislocations to quantum glasses; but none of the proposed models seems able to capture the whole phenomenology of supersolidity in solid ^{4}He [10]. Thus, independent of the very relevant issue of intrinsic or extrinsic defects, the knowledge of the properties of defects in this system is one of the main goals of the present theoretical investigations on supersolidity in this system.

From the theoretical point of view the method of choice to investigate a strongly interacting quantum system like solid ^{4}He is Quantum Monte Carlo (QMC) simulations. Nowadays a number of studies on defected solid ^{4}He systems studied by means of QMC techniques are present in literature [18,19, 20,21,22,23,24,25,26,28,29,30,31,32,33,34,35,36,37,38]. Crystals with defects can be simulated with an appropriate choice of the simulation box (SB) and the number of particles such that, combined with the use of periodic boundary conditions (PBC), the MC sampling is constrained to configurations which host the desired defect. When PBC are not able to stabilize the

defect, one can constrain (or fix) the degrees of freedom of a number of atoms surrounding the defect of interest [30]. These constraints on the configurational space, if judiciously implemented, usually do not prevent the study of the physical properties of the (defected) system; as an example, the binding energy of a ^{3}He atom to dislocation cores turned out to be in agreement with experimental data [31]. A distinct issue is the investigation of the nature (defected or not) of the ground state of the extended system; in this case, such strategies are not straightforwardly convincing and some doubt remains on the level of confidence to give to the results: beside the finite size effects, one also has to check to what extent the results are influenced by the choice of boundary conditions. In fact, the constraint imposed by the PBC on the configurational sampling of a crystalline solid is both stronger and subtler than what is usually believed, due to commensurability effects between crystal unit cell and SB [40].

In the present paper we address two topics. The first is to study if it is true that vacancies are not a viable route to supersolidity because multiple vacancies coalesce and lead to phase separation [35]. The second topic is to study what we learn from quantum simulations by studying large systems *without* using PBC. On the first topic we review and extend a systematic study of many vacancies (up to 30) in two-dimensional (2D) solid ^{4}He based on exact $T = 0$ K quantum simulations. A pure 2D solid is of interest as a simple model for out of registry solid ^{4}He adsorbed on planar substrates, and new experimental investigations [39] are under way to answer the question of whether a supersolid state is present also in adsorbed ^{4}He. In no case do we find that the crystalline order is unstable, at least as long as the concentration of vacancies is below 2.5%. Multiple vacancies were found highly correlated with a tendency to form linear structures. Actually, when $n_v > 10$ vacancies transform themselves into dislocations. This resembles the behavior of multiple vacancies in classical solids at low temperature [41]. In our quantum crystal such dislocations are very mobile, allowing exchange of particles across the system; in fact, we find ODLRO in the one-body density matrix ρ_1 computed for the finite simulated system. In presence of disorder, this gives the possibility of establishing a well defined phase [42], at least locally, in the extended system. Should the exact ground state of ^{4}He in 2D not be an ideal perfect crystal, our results imply that the zero–point disorder does not consist of vacancies but of dislocations and that the extended system could be supersolid.

As second topic we study systems *free* of PBC by confining the ^{4}He atoms in a finite region of space by an external potential. The main aim is to investigate the true nature of the ground state, i.e. to determine if defects restrict themselves in the interfacial region near to the confining potential, triggered by the mismatch between the confining geometry and the triangular lattice of 2D solid ^{4}He, or if defects also permeate the inner region. We give evidence that once the equilibrium is reached, the defects, even if initially placed in the center of the system, essentially restrict themselves in the interfacial region, leaving the inner region a regular triangular lattice. Moreover, we find that the inner crystal is compatible with the ideal crystal simulated in a periodically repeated box (i.e. in standard simulations with PBC). Given the size of

the studied systems, this gives an upper bound on the concentration of any ground state defects, which must be below 3×10^{-3}.

The paper is organized as follows: Sec. 2 deals with the *exact* $T = 0$ K shadow path integral ground state (SPIGS) method and the definition of quantities used in measuring the crystal disorder. Details on the simulations and our results on the periodically repeated crystal are presented in Sec. 3. Sec. 4 contains a discussion on the issue of zero–point defects and on the influence of using PBC. Sec. 5 contains details on the simulations and results on the confined 2D crystal. Conclusions are given in Sec. 6.

2 Simulation details

The SPIGS method: We study solid ^{4}He via *exact* simulation methods based on the Shadow Path Integral Ground State (SPIGS) [21,22] method. SPIGS is an extension of the Path Integral Ground State (PIGS) [43] method. The aim of PIGS is to improve a variationally optimized trial wave function ψ_T by constructing, in the Hilbert space of the system, a path which connects the given ψ_T with the exact lowest energy wave function of the system, ψ_0, constrained by the choice of the number of particle N, the geometry of the SB, the boundary conditions and the density ρ. During this "path", the correct correlations among the particles arise through the "imaginary time evolution operator" $e^{-\tau \hat{H}}$, where $\hat{H}$ is the Hamiltonian operator. For a large enough τ, an accurate representation for the lowest energy state wave function is given by $\psi_\tau = e^{-\tau \hat{H}} \psi_T$, which can be written analytically by discretizing the path in imaginary time; this maps the quantum system into a classical system of open polymers [43]. An appealing feature peculiar to the PIGS method is that, in ψ_τ, the variational ansatz acts only as a starting point, while the full path in imaginary time is governed by $e^{-\tau \hat{H}}$, which depends only on the Hamiltonian operator. We have recently shown that ψ_τ does not need to be a variational optimized wave function: PIGS results for large enough τ are unaffected by the choice of ψ_T both in the liquid and in the solid phase [13,44] thus providing an unbiased exact $T = 0$ K QMC method. Within SPIGS a shadow wave function (SWF) [45,46] is taken as ψ_T and this choice was shown to greatly accelerate convergence to ψ_0. Another feature of the SPIGS method is that it recovers the solid phase via a spontaneously broken translational symmetry [21,22], like in Path Integral Monte Carlo (PIMC), and there is no constriction on the atomic positions, so it is particularly useful in studying crystals with defects.

Measuring crystal order and fluctuations: We check the presence of crystalline order by monitoring the static structure factor for the presence of Bragg peaks and, via a Delaunay triangulation [35] (DT) of the sampled configurations, we compute the particle coordination number in order to estimate the amount of local disorder in the system [47]. In an ideal perfect 2D triangular crystal, with the atoms in their equilibrium positions, each atom is linked to 6 other atoms in the DT. Atoms with coordination number not equal to 6 are then a measure of fluctuations and of local disorder in the crystal. In periodically repeated systems in 2D one proves a conservation law

for the coordination numbers:

$$\sum_{i=3}^{5}(6-i)N_i = \sum_{i+7}^{\infty}(i-6)N_i \tag{1}$$

where N_i is the number of $i-$coordinated atoms, so that we can consider only N_i with $i < 6$. Since it is always verified that $N_3 = 0$, the quantity $\tilde{X}_d = 2N_4 + N_5$ is usually taken as an estimate of local disorder in the system [48]. However, even in an ideal (defect-free) 2D quantum crystal the coordination is 6 only on the average: atoms are not always 6-fold coordinated due to their large zero–point motion. Then, a more useful quantity measuring the net amount of disorder in a crystal with n_v vacancies, for instance, is the difference between the observed $\tilde{X}_d$ and that of the corresponding ideal perfect crystal:

$$X_d = (2N_4 + N_5)_{n_v} - (2N_4 + N_5)_{n_v=0}. \tag{2}$$

We have studied also the orientational order parameter Ψ_6 to quantitatively characterize the quality of crystalline structures. The local order parameter that measures the degree of 6-fold-orientational ordering is defined [49] as

$$\psi_6(\mathbf{r}_k) = \frac{1}{n(k)} \sum_{j=1}^{n(k)} e^{i6\theta_{kj}} \tag{3}$$

where θ_{kj} is the angle between the vector $\mathbf{r}_k - \mathbf{r}_j$ and a fixed direction in the plane (chosen here to be the positive x direction) and the sum over j extends over all $n(k)$ nearest-neighbor of the k-th atom as provided by the DT. The global order parameter associated with bond-orientational order is then obtained as an average over all particles

$$\Psi_6 = \frac{1}{N} \sum_{k=1}^{N} \psi_6(\mathbf{r}_k) \tag{4}$$

In a static ordered triangular solid, we have $n(k) = 6$ and θ_{kj} is a multiple of $\pi/3$ for all $j = 1, \ldots, 6$. In such a case, $| \langle \Psi_6 \rangle | = 1$ and the plot of $\langle \Psi_6 \rangle$ on a complex plane will result in a single spot on a circumference with unit radius. Because of the fluctuations due to the zero–point motion we expect that, even in the perfect crystal, this spot will be broadened along the circumference and toward the center. In the presence of vacancies or other defects we expect significantly less orientational order and the plot of Ψ_6 should extend over a larger portion of the circle (in the limiting case of the liquid system, it turns in a distribution centered around the origin).

3 Results: periodically replicated crystal

Recently we have performed the first systematic study of multiple vacancies in two dimensional (2D) solid ^{4}He [35]. Dealing with low temperature
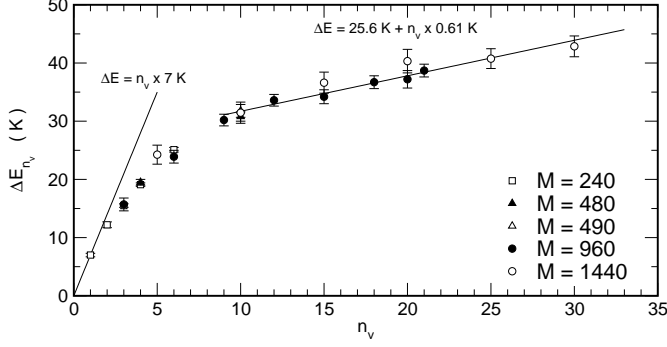
Fig. 1 Defect formation energy ΔE_{n_v} at constant density as a function of n_v in 2D solid ^{4}He at $\rho = 0.0765$Å^{-2} computed in boxes with different lattice site numbers M. Dashed lines are linear fit to the data.

properties, ^{4}He atoms are described as structureless zero–spin Bosons inter-acting through the standard HFDHE2 Aziz potential [50]. From the computed equation of state we found the freezing and the melting densities to be, respectively, $\rho_f = 0.0672$ Å^{-2} and $\rho_m = 0.0724$ Å^{-2}. In our SPIGS computation for the periodically repeated system we have used the pair-product approximation [51] for the imaginary time projector; as a compromise between good accuracy and reasonable computational effort $\delta\tau$ has been set to 1/40 K^{-1}. A total projection imaginary time $\tau = 0.775$ K^{-1} ensures convergence to the ground state. We have simulated a 2D crystal at densities slightly above the melting density. The geometry of the SB is such that it is compatible with a regular triangular lattice and the study has been performed with $M = 240$, 480, 960 and 1440 *lattice positions* and PBC were applied in all directions. When $N = M$ we have an ideal ordered crystal. By removing atoms from the initial ordered configuration we can study a system with a variable $n_v = M - N$ number of putative vacancies. n_v ranged from 0 to 30, with a maximum vacancy concentration $x_v = n_v/N$ of 0.025. For larger values of x_v the crystalline order is lost. After removing n_v particles from the starting ideal ordered configuration the dimensions of the SB were rescaled to restore the original crystal density ρ. As a test of convergence we performed simulations starting from different positions of the n_v vacancies.

The crystalline order is stable for all the cases considered and the properties of the system display a dependence on n_v rather than on x_v. Both the diagonal and the off-diagonal properties were found to exhibit a double regime behavior[35]. For $n_v < 6$ the defects are easily identified in the snapshots of the atomic positions and the defect formation energy ΔE_{n_v} is found to be monotonic and systematically sublinear with n_v. This is consistent with the presence of an attractive interaction among vacancies (as confirmed by the vacancy-vacancy correlation function [35]). For $n_v \gtrsim 10$ ΔE_{n_v} becomes linear in n_v, with a cost of 0.61K for each additional vacancy, i.e. the formation energy for an additional vacancy in this regime costs about ten times less than the energy (7 K) required for a single vacancy (see Fig. 1). A similar double regime behavior has been found also in the static structure factor

and in the amount of disorder X_d. For $n_v < 6$ the main Bragg's peaks are found as sharp as in the perfect crystal but with a decreased height and X_d is found to increase with n_v (as expected for an increasing disorder). When $n_v \gtrsim 10$ the behavior is quite different: the main Bragg's peaks are slightly broadened but with an integrated intensity that is almost independent of n_v and also X_d does not depend on n_v. By looking to the sampled configurations we realized that multiple vacancies for $n_v \lesssim 6$ are highly correlated with a preference to form fluctuating linear structures. On the other hand when $n_v \gtrsim 10$ the vacancies inserted in the initial configuration lose their identity and transform themselves into quantum dislocations [35]. In the range 6–10 there is a crossover between the two regimes. We have now analyzed such multiple vacancy systems in terms of the orientational order parameter Ψ_6. Ψ_6 also displays a similar double regime behavior. Some examples of the obtained results are reported in Fig. 2. By comparing the result of $\langle \Psi_6 \rangle$ in the ideal perfect crystal (Fig. 2a) with the results for the crystal with 1 vacancy (Fig. 2b), 4 vacancies (Fig. 2c) and 10 putative vacancies (which equilibrate into dislocations, Fig. 2d), one can see that, in the cases when disorder is present, $\langle \Psi_6 \rangle$ fills more of the complex plane far from the point $\Re[\langle \Psi_6 \rangle]=1$ on the real axis with respect to the perfect crystal case. However, in going from the 4 vacancies to the dislocations case, the signal of disorder decreases, inverting the trend from 1 to few vacancies; again this is a signature of the double regime behavior found in monitoring other quantities. An interstitial (Fig. 2e) gives a distinct signature of disorder with respect to that of a vacancy; 4 interstitials give a disorder map in $\langle \Psi_6 \rangle$ that is less extended than that for a single interstitial, showing some cooperative correlations also among interstitials. In fact, by looking at the DT of the sampled configurations we can recognize the presence of dislocations also in this case.

This double regime is found also in the large distance behavior of the one-body density matrix ρ_1. For small n_v, as n_v increases, the plateau in the ρ_1 tail, which is the signature of ODLRO, decreases, and this can be interpreted as an effect of the vacancy–vacancy interaction. Should this trend continue into the large n_v regime, no ODLRO could be present in the thermodynamic limit, implying that an extended crystal with vacancies would not be super-solid. However we find a different behavior: for $n_v \gtrsim 10$ the plateau in the large distance tail of ρ_1 is restored (see Fig. 3) mainly due to the ability of the dislocation cores to transfer particles among them. In fact, dislocations turn out to be very mobile and are able to induce exchanges of particles across the whole system, which is a necessary condition for ODLRO. Unfortunately, no size scaling analysis on ρ_1 has been done yet in the dislocation regime because of the prohibitive computational cost of off-diagonal simulations of systems large enough to accommodate a large number of dislocations. In Fig. 3a and Fig. 3b one sees the presence of ridges in the tail of ρ_1. As discussed in detail in Ref. [35], these ridges are due to commensuration effects between dislocations and SB size.

An important question is the behavior of many vacancies in a 3D crystal. Based on finite temperature simulations, statements in the literature [25] are found that in presence of many vacancies the crystal becomes unstable
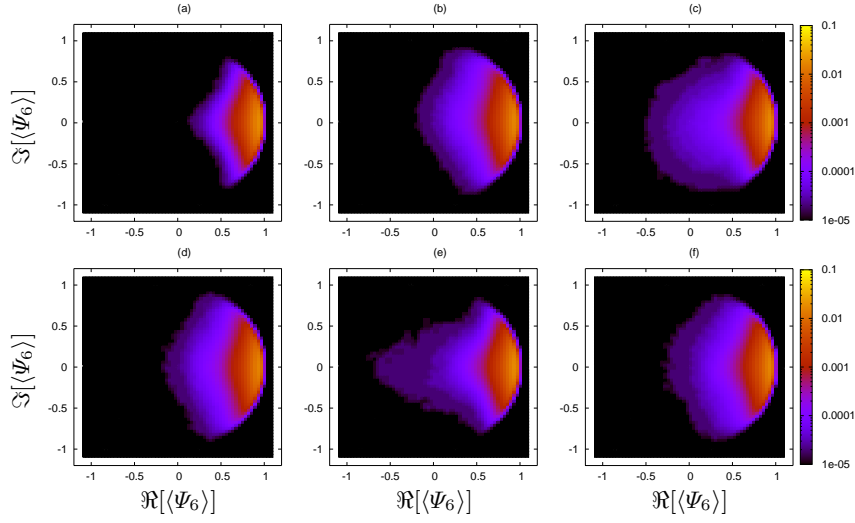
Fig. 2 (Color online) Intensity plots of the probability of Ψ_6 on the complex plane for a bulk 2D ^{4}He crystal at $\rho = 0.079$ Å^{-2}, for the (a) ideal perfect crystal with $N = 572$, (b) crystal with a vacancy ($N = 571$), (c) crystal with 4 vacancies ($N = 568$) (d) crystal with dislocations ($n_v = 10$) with $N = 562$, (e) crystal with an interstitial ($N = 573$), (f) crystal with 4 interstitials (dislocations) with $N = 576$. Note the logarithmic intensity scale.
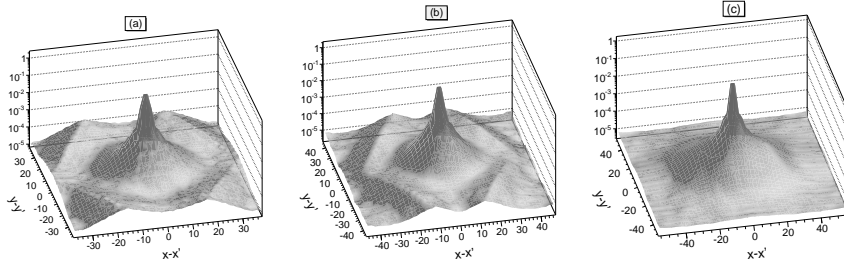

Fig. 3 One–body density matrix $\rho_1(\mathbf{r}, \mathbf{r}')$ in the $x - x', y - y'$ plane computed in a defected ^{4}He 2D crystal ($n_v = 10$) at $\rho = 0.0765$Å^{-2} for different numbers of lattice sites M: (a)$M = 480$ (b) $M = 700$ (c) $M = 960$.

against separation into a vacancy–rich and a crystalline vacancy–free phase. We found no such instability at $T = 0$ K not only in 2D but also in 3D for as many as 98 vacancies as discussed in Ref. [35].

4 Periodic boundary conditions, the crystalline state and the issue of zero–point defects in solid ^{4}He

All simulations deal with a finite number N of particles and, in order that such finite size systems mimic a bulk system, PBC turn out to be very useful. In a fluid system the extrapolation to the bulk limit of the simulation results for short range properties is rather straightforward, unless one is close to a critical point, because the results depend smoothly on N. The situation is more complex for a crystalline solid because simulated properties are affected also by commensuration effects between the SB and the crystalline unit cell. As an example of this consider the following. The stable phase of solid ^{4}He at low T and pressure is the hcp crystalline state. However, from exact quantum simulations of realistic models of ^{4}He it turns out that all three phases hcp, fcc and bcc are stable (with a different value of the energy) for a suitable choice of the SB geometry and of N [23]; i.e. the average density, ρ, has to be large enough and the sides of the SB have to be integer multiples of the sides of the unit cell of the crystal under study. Finite size scaling for a given phase is performed by considering a special set of numbers of particles, for instance 180, 448, 900 for hcp, but this explores a special set of states predetermined by the choice of SB and N. The conclusion is that finite size scaling is very special in a crystalline solid and it does not give an unbiased estimate of the properties of the bulk system. One might think that a way out of such a limitation is to start from a disordered configuration and let the system crystallize into the preferred state. The problem is that PBC again constrain the system. In fact, compatibility between a crystal lattice and PBC for a given SB is present only for certain orientations of the crystal axis with respect to the axis of the SB. The spontaneous crystallization of the particles has essentially zero probability to pick up such special orientations and, in fact, computer experiments [52] show that crystallization does indeed take place, but the crystal axis take arbitrary orientations with respect to the SB so that the crystalline order is deformed in order to comply with the PBC.

For similar reasons one cannot expect to see during the computation the spontaneous appearance of a vacancy. An objection [25,12,26] to the presence of ground state vacancies is that such defects cost large energies, quantum simulations [18,21,25,26] agree on a value of order of 15 K in 3D at the melting density, so that no defect should be present at low T. This, however, fails to recognize that those simulations addressed specifically the question of the energy cost of a vacancy as an excited state and this is a separate question from the presence of vacancies in the ground state. It is instructive to consider the lattice gas model introduced by Mullin [27]. This model displays a liquid phase, a normal solid and a supersolid phase. In the supersolid state the occupation probability of a lattice site is less than unity and delocalized vacancies are present (more precisely vacancy-interstitial pairs) as an effect of zero point motion. Yet, the excitation spectrum has a gaped vacancy-interstitial branch. Anderson [15] has argued that in a Bose quantum crystal a unit population of a lattice site is incompatible with quantum mechanics

and that some vacancies have to be present in a highly quantum system like solid [4]He.

One way to address the question of the presence of vacancies in the ground state of solid [4]He is to proceed in a way similar to what is done in classical statistical mechanics in computing the equilibrium concentration of vacancies in a classical solid. The method is based on considerations of a macroscopic system, not the one that is simulated, and a basic assumption is that vacancies can be treated as weakly interacting objects. Within variational theory, using a SWF as ground state, a finite concentration x_v of zero–point vacancies has been found with $x_v \simeq 1.4 \times 10^{-3}$ at melting density [53]. This is a sizeable concentration not too far from the actual experimental upper bound. Extension of this computation to the case of the exact ground state is a difficult and open problem also because one has to take into account that vacancies are strongly interacting and tend to transform themselves into dislocations, at least in 2D, as discussed in the previous section.

Another approach to study the presence of ground state vacancies is to get away from PBC by considering a confined system. This is the topic of the next section.

5 Confined crystal

Specific simulation details: In the study of confined systems we have opted for an implementation of the worm algorithm [11] with a fixed number of particles and for the pair-Suzuki approximation [44] for the imaginary time propagator $e^{-\delta\tau\hat{H}}$; $\delta\tau$ has been set to $1/360$ K^{-1} and the total imaginary projection time $\tau = 0.775$ K^{-1} is equal to the value used in the simulations of the periodically replicated crystal.

The confining potential has been chosen to be circular symmetric so that all directions are equivalent and, in addition, this ensures minimal mismatch with the crystalline triangular structure so that the interfacial region should be minimal. Since we are not interested in simulating any specific confinement, we have chosen the confining potential V_{ext} to be only repulsive and to represent an hypothetical surrounding infinite [4]He bulk crystal at density ρ_{ext} with the atoms considered as a continuum. Then V_{ext} reads

$$V_{\text{ext}}(r) = \begin{cases} V_{\text{LJ}}(R-r) - V_{\text{LJ}}(R-r_{\min}) & R - r_{\min} < r < R \\ 0 & r < R - r_{\min} \end{cases} \tag{5}$$

where R is the radius of the confining potential and V_{LJ} is obtained by integrating a standard 12-6 Lennard-Jones potential on the half-plane:

$$V_{\text{LJ}}(r) = \frac{3\pi\varepsilon\sigma^6}{8}\rho_{\text{ext}}\left[\left(\frac{21\sigma^6}{80r^{10}}\right) - \left(\frac{1}{r^4}\right)\right] \tag{6}$$

and $r_{\min}$ is the position of the minimum in V_{LJ}. As ε and σ we use the typical Lennard-Jones parameters for [4]He, i.e. 10.22 K and 2.556 Å respectively, and ρ_{ext} is set to 0.0765Å^{-2}. Such a confining potential fails in accounting for the confining curvature, but the curvature effect is small for the large
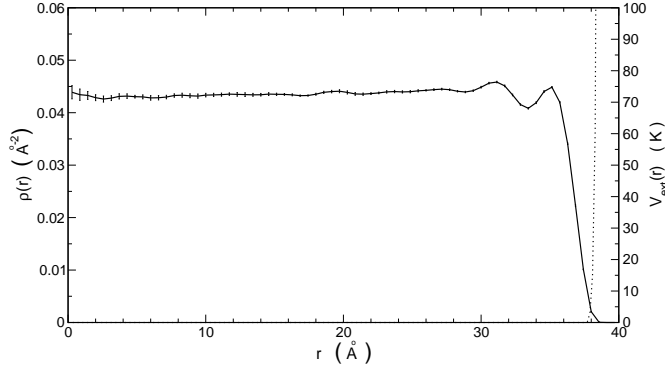
Fig. 4 (solid line) Radial density profile, $\rho(r)$, for a system with $N = 187$ and $R = 40.0$ Å. (dotted line) Confining potential, $V_{\text{ext}}(r)$

values of the radius R here considered. The initial configuration is obtained by building a regular triangular lattice at a density ρ_S and discarding all the particles falling out the disk of radius $R - r_{\text{min}}$. The number of particles inside this disk is referred to as $N_0(\rho_S)$. If ρ_S is below a certain value the atoms quickly lose the initial crystalline order and the system evolves into a liquid state. As an example, in Fig. 4 the case of a confining potential with $R = 40$ Å and $N_0(\rho_S) = 187$ ($\rho_S = 0.0435$ Å^{-2}) is shown. From the plot of the radial density profile it is evident that the confinement gives rise to an interfacial region that covers an annulus whose thickness is not larger than about 8 Å. By increasing the number of particles at fixed radius R, we find that the particles become more and more localized and beyond a certain value of N the solid order becomes visually evident. For the solid phase, such interfacial region is expected to be thicker because of the effect of the mismatch between the triangular geometry of the confined crystal and the circular one of the confining potential. We have considered different values of the radius R and we find that the interfacial region never penetrates more that 15 Å inside the system.

In order to promote the presence of defects in the inner region, additional simulations are performed by subtracting or inserting particles at random positions from an equilibrated configuration for the system with $N_0(\rho_S)$ particles. For the confined crystal the quantity $\tilde{X}_d$, introduced in the previous section, is no longer appropriate because of the lack of a conservation law like the one in (1). In place of $\tilde{X}_d$, as an estimate of the local disorder, we use the density $\rho_{\not{6}}$ of the particles that are miscoordinated, i.e. with coordination number different from 6.

Results: We have considered three different values for R, 44.6 Å, 54.6 Å and 64.6 Å, that give rise, respectively, to $N_0(\rho_S) = 433$, 685 and 931 ^{4}He atoms when the starting configuration is obtained by cutting from an ideal triangular lattice at $\rho_S = 0.0765$ Å^{-2}. When equilibrated, the system is solid with an average density ρ_{av} slightly different from ρ_S because of relaxations of the atoms in the confining potential (ρ_{av} are reported in the legend of Fig. 6). In the present paper we discuss mainly the case of the intermediate
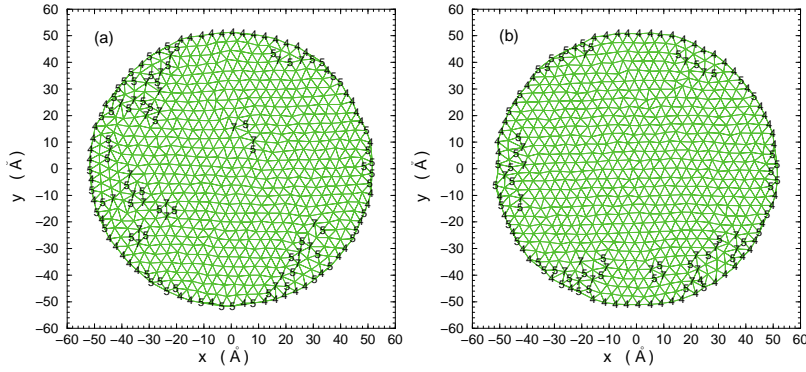
Fig. 5 (color online). Delaunay triangulation of typical configurations of a 2D confined ^{4}He crystal with $N = 671$ and $R = 54.6$ Å (a) after few hundreds Monte Carlo steps from the random removal of 14 particles from an equilibrated configuration of the system with $N = N_0(\rho_S)$ and (b) when equilibrium has been reached. We report the coordination number for atoms only when different from 6. The couple 5–7 indicates a dislocation core in 2D and the clumps of two 5 and two 7 indicate bound pairs of dislocations.

radius value $R = 54.6$ Å. In addition to the "magic" number $N_0(\rho_S) = 685$ we have considered also an initially "defected" crystal by changing the number of particles. From an equilibrated configuration with 685 ^{4}He atoms we have removed 14 particles at random positions obtaining a system with $N = 671$ particles, and we have also randomly inserted 14 particles in order to obtain a system with $N = 699$ particles. In the case of such initial defected state the MC evolution has two stages. At first, after a few hundred MC steps, the crystal relaxes around the injected defects and we have a confined solid with defects (vacancies or interstitials) that are present also in the inner region. In Fig. 5 (a) the DT of one typical configuration in this initial evolution for the $N = 671$ system is shown. At a later stage of the MC evolution, the system reaches an equilibrium state with no sign of defects recorded in the inner region (see Fig. 5 (b)). This is confirmed also by the density of miscoordinated particles $\rho_{\not{6}}$. From the plot in Fig. 6 it is easy to recognize in the system with $R = 54.6$ and 64.6 Å a disk of about 30 Å radius in which $\rho_{\not{6}}$ is essentially compatible with the expected value in periodically repeated ideal crystals at similar densities. In Fig.6 $\rho_{\not{6}}(r)$ for a periodically repeated crystal with one vacancy is also shown. Its value is about 40 times larger of that of the system without a vacancy. It is clear that the values of $\rho_{\not{6}}(r)$ in the inner region of the confined system are incompatible with the presence of such defect.

The suggestion of a defect-free inner region is supported also by the following argument. Consider a periodically repeated crystal. As discussed in Sec. 2, even in the ideal perfect crystal there is a finite probability to find miscoordinated particles due to the zero–point motion. Since this is a fluctuation effect, we might expect the permanence time $t_{\not{6}}$, i.e. the mean number of MCS in which a given ill coordinated particle remains ill coordinated, is smaller in an ideal perfect crystal compared with the case of a crystal with a
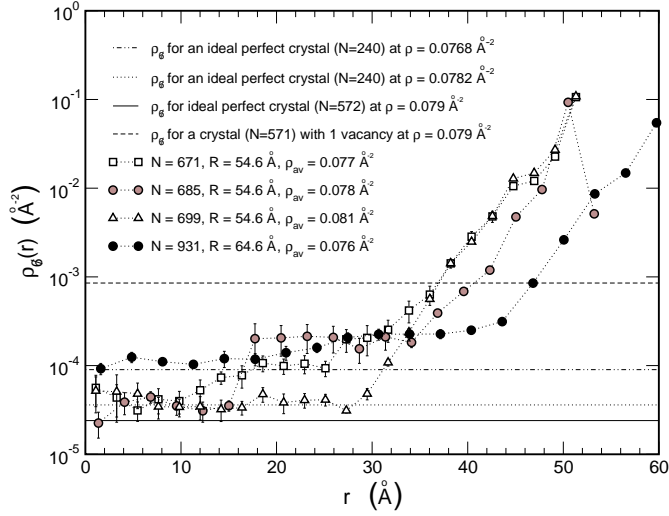
Fig. 6 Local densities, $\rho_{\cancel{6}}(r)$, of particles with coordination different from 6 as function of radial distance for a number of 2D confined ^{4}He crystals. For comparison with the values of bulk 2D ^{4}He crystals at similar densities are also shown (see legend).

vacancy, because the vacancy is a permanent defect whose dynamics is governed by the rate of vacancy jump. Indeed, at density $\rho = 0.77$ Å^{-2} we find $t_{\cancel{6}} = 4.0$ MCS for the periodically repeated ideal perfect crystal and $t_{\cancel{6}} = 9.5$ when a vacancy is present. A similar computation for the confined system and considering only particles with $r < 30$ Å gives $t_{\cancel{6}} = 3.0$, 2.7 and 2.8 in the systems with $N = 671$, 685 and 699, respectively. Thus not only is the inner region free of defects, but it turns out to be somehow less fluctuating than the system with PBC, presumably due to the stabilizing effect of the confining potential.

Also the study of the orientational order parameter Ψ_6 corroborates the finding that no defects permeate into the inner region of the confined crystal. From the plots Fig. 7 it is evident that within 30 Å from the center the results for $\langle \Psi_6 \rangle$ in the confined system with $R = 54.6$ are close to the results obtained in the periodically repeated ideal crystal reported in Fig. 2 for the three numbers of particles, $N = 671$, 685 and 699. In the range 30–40 Å there is a crossover to the outer region of width ~ 15 Å strongly perturbed by the confining potential.

In conclusion, our study of a confined system shows that the inner region is free of defects like vacancies or interstitials; if defects are present in the initial configuration these anneal away and go to the interfacial region. Since our system is finite, our computation allows to give only an upper bound to the concentration of ground state defects. Taking into account that the inner region has a radius of 35 Å in which the average number of ^{4}He atoms is about 300, this upper bound is 3×10^{-3}. We notice that this upper bound is above the estimated concentration of vacancies given by a SWF (in 3D) [53].
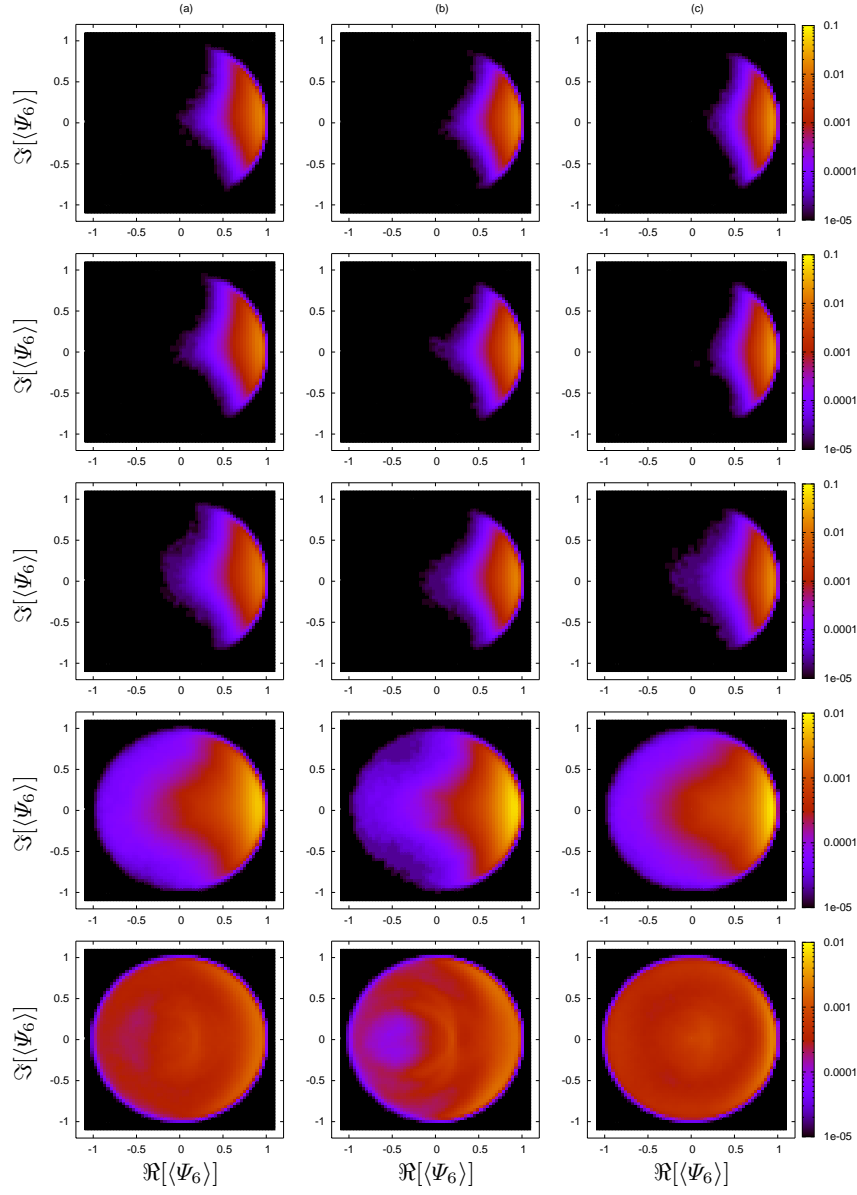
Fig. 7 (Color online) Intensity plots of the probability of Ψ_6 on the complex plane computed for different annular shells ($r_{min} \leq r < r_{max}$) for 2D confined ^{4}He crystals with $R = 54.6$ Å. (column a) $N = 671$ (column b) $N = N_0(\rho_S) = 685$ (column c) $N = 699$; (first row) $0 \leq r < 20$ Å (second row) $20 \leq r < 30$ Å (third row) $30 \leq r < 40$ Å (fourth row) $40 \leq r < 50$ Å (fifth row) $50 \leq r < R$ Å. Note the logarithmic intensity scale.

6 Conclusions

The issue of ground state defects in crystalline ^{4}He is still debated. In 3D we have studied up to 98 vacancies in system of 2548 atoms and in 2D up to 30 vacancies in a system of 1410 atoms and in all cases the crystalline order, as studied by different methods, turns out to be stable as long as the concentration of vacancies is below about 2.5%. Multiple vacancies are *not* weakly interacting though, they display signature of strong interaction. The most detailed study has been performed in 2D. For up to 6 vacancies one find a tendency for the vacancies to form linear structures. Starting from 10 vacancies, in the relaxed state such vacancies cannot be identified anymore but the system displays the presence of fluctuating dislocations. This suggests that should ground state defects be present in solid ^{4}He, such defects would be dislocations and not vacancies.

We have stressed the role of periodic boundary conditions in quantum simulations of a crystalline solid. The computed quantities are affected not only by the usual size effects, but also by commensuration effects between the simulation box and the crystalline lattice. We have investigated solid ^{4}He in 2D without the use of PBC by confining the atoms via an external potential. We find that the effects of the confining potential extend mainly in a layer of width of order of 15 Å, inside this interfacial region the atoms display a crystalline order similar to that of a bulk crystal and we find no evidence for the presence of defects. If defects like vacancies or interstitials are introduced in the initial state, such defects migrate to the interfacial region leaving the inner region free of defects. Taking into account the finite size of the system, this allows us to put an upper limit of 3×10^{-3} to the concentration of zero–point defects.

Many extensions of the present study can be foreseen. A stronger bound on the concentration of zero–point defects will require the study of larger systems. The walls of a real container are never smooth and it will be interesting to see how the properties of the systems are affected by assuming a confining potential not as smooth as the one used in the present study. The study of confined system in 3D should be interesting but it is hindered by the very large number of particles needed in order to get relevant results.

References

1. O. Penrose and L. Onsager, *Phys. Rev.* **104**, 576 (1956).
2. A.F. Andreev and I.M. Lifshitz, *Soviet Physics JETP* **29**, 1107 (1969).
3. G.V. Chester, *Phys. Rev.* A **2**, 256 (1970).
4. M. W. Meisel, *Physica B* **178**, 121 (1992).
5. E. Kim and M.H.W. Chan, *Nature* **427**, 225 (2004); *Science* **305**, 1941 (2004); *Phys. Rev. Lett.* **97**, 115302 (2006).
6. A.J. Leggett, *Phys. Rev. Lett.* **25**, 1543 (1970).
7. N.V. Prokof'ev, *Adv. Phys.* **56**, 381 (2007).

8. S. Balibar and F. Caupin, *J. Phys.: Condensed Matter* **20**, 173201 (2008).
9. D.E. Galli and L. Reatto, *J. Phys. Soc. Jpn.*, **77**, 111010 (2008).
10. S. Balibar, *Nature* **464** 176 (2010).
11. Boninsegni, N. V. Prokof'ev, and B. V. Svistunov, *Phys. Rev. Lett.* **96**, 105301 (2006).
12. B. K. Clark and D. M. Ceperley, *Phys. Rev. Lett.* **96**, 105302 (2006).
13. E. Vitali, M. Rossi, F. Tramonto, D.E. Galli and L. Reatto, *Phys. Rev. B* **77**, 180505(R) (2008).
14. P. W. Anderson, W. F. Brinkman, and D. H. Huse, *Science* **310** 1164 (2005).
15. P. W. Anderson, arXiv:1111.1707.
16. R. O. Simmons, *J. Phys. Chem. Solids* **55**, 895 (1994).
17. R. O. Simmons and R. Blasdell, presented at APS March Meet., Denver, Colorado, 2007.
18. F. Pederiva, G.V. Chester, S. Fantoni and L. Reatto, *Phys. Rev. B* **56**, 5909 (1997).
19. D.E. Galli and L. Reatto, *J. Low Temp. Phys.* **124**, 197 (2001).
20. D.E. Galli and L. Reatto, *Phys. Rev. Lett.* **90**, 175301 (2003).
21. D.E. Galli and L. Reatto, *Mol. Phys.* **101**, 1697 (2003).
22. D.E. Galli and L. Reatto, *J. Low Temp. Phys.* **136**, 343 (2004).
23. D.E. Galli and L. Reatto, *J. Low Temp. Phys.* **134**, 121 (2004).
24. D.E. Galli and L. Reatto, *Phys. Rev. Lett.* **96**, 165301 (2006).
25. M. Boninsegni, A.B. Kuklov, L. Pollet, N.V. Prokof'ev, B.V. Svistunov and M. Troyer, *Phys. Rev. Lett.* **97**, 080401 (2006).
26. B.K. Clark and D.M. Ceperley, *Comp. Phys. Comm.* **179**, 82 (2008).
27. W.J. Mullin, *Phys. Rev. Lett.* **26**, 611 (1971).
28. L. Pollet, M. Boninsegni, A.B. Kuklov, N.V. Prokof'ev, B.V. Svistunov, and M. Troyer, *Phys. Rev. Lett.* **101**, 097202 (2008).
29. L. Pollet, M. Boninsegni, A.B. Kuklov, N.V. Prokof'ev, B.V. Svistunov, and M. Troyer, *Phys. Rev. Lett.* **98**, 135301 (2007).
30. M. Boninsegni, A.B. Kuklov, L. Pollet, N.V. Prokof'ev, B.V. Svistunov and M. Troyer, *Phys. Rev. Lett.* **99**, 035301 (2007).
31. P. Corboz, L. Pollet, N.V. Prokof'ev and M. Troyer, *Phys. Rev. Lett.* **101**, 155302 (2008).
32. S.G. Soyler, A.B. Kuklov, L. Pollet, N.V. Prokof'ev and B.V. Svistunov, *Phys. Rev. Lett.* **103**, 175301 (2009).
33. R. Pessoa, M. de Koning, and S. A. Vitiello, *Phys. Rev. B* **80**, 172302 (2009).
34. R. Pessoa, S.A. Vitiello, and M. de Koning, *Phys. Rev. Lett.* **104**, 085301 (2010).
35. M. Rossi, E. Vitali, D.E. Galli and L. Reatto, *J. Phys.: Condens. Matter* **22**, 145401 (2010)
36. Y. Lutsyshyn, C. Cazorla, G.E. Astrakharchik, and J. Boronat, *Phys. Rev. B* **82**, 180506(R) (2010).
37. Y. Lutsyshyn, C. Cazorla and J. Boronat, *J. Low Temp. Phys.* **158**, 608 (2010).
38. R. Rota and J. Boronat, *Phys. Rev. Lett.* **108**, 045308 (2012).
39. Y. Shibayama, H. Fukuyama and K. Shirahama, *J. Phys.: Conf. Ser.* **150**, 032096 (2009).
40. W.C. Swope, H.C. Andersen, *Phys. Rev. A* **46**, 4539 (1992).
41. W. Lechner and C. Dellago, *Soft Mat.* **5**, 2752 (2009).
42. P.W. Anderson, *Phys. Rev. Lett.* **100**, 215301 (2008).
43. A. Sarsa, K. E. Schmidt, and W. R. Magro, *J. Chem. Phys.* **113**, 1366 (2000).
44. M. Rossi, M.Nava, L. Reatto and D.E. Galli, *J. Chem. Phys.* **131**, 154108 (2009).
45. S.A. Vitiello, K. Runge and M.H. Kalos, *Phys. Rev. Lett.* **60**, 1970 (1988).
46. S. Moroni, D.E. Galli, S. Fantoni and L. Reatto, *Phys. Rev. B* **58**, 909 (1998).
47. Particle configurations at fixed imaginary time have very strong fluctuations due to zero–point motion; in order to average over such fluctuations, as particle position we take the center of mass of the configurations of a suitable number of inner time–slices of the polymer. In the reported calculations this corresponds to an imaginary time interval of about 0.9 K^{-1} out of $2\tau = 1.55$ K^{-1}.
48. B. Krishnamachari and G.V. Chester, *Phys. Rev. B* **61**, 9677 (2000).

49. J. P. McTague, D. Frenkel, and M. P. Allen, in *Ordering in Two Dimensions*, edited by S. K. Sinha (North-Holland, Amsterdam, 1980).
50. R.A. Aziz, V.P.S. Nain, J.S. Carley, W.L. Taylor and G.T. McConville, *J. Chem. Phys.* **70**, 4330 (1979).
51. D.M. Ceperley, *Rev. Mod. Phys.* **67**, 279 (1995).
52. F. Pederiva, A. Ferrante, S. Fantoni, and L. Reatto, *Phys. Rev.* B **52**, 7564 (1995).
53. M. Rossi, E. Vitali, D.E. Galli and L. Reatto, *J. Low Temp. Phys.* **153**, 250 (2008).